THE JOURNAL OF PHYSICAL CHEMISTRY B

ARTICLE

pubs.acs.org/JPCB

On the Viscosity of Pyridinium Based Ionic Liquids: An Experimental and Computational Study

Isabel Bandrés,[†] Rafael Alcalde,[‡] Carlos Lafuente,[†] Mert Atilhan,[§] and Santiago Aparicio*[,‡]

[†]Departmento de Química Física, Universidad de Zaragoza, Zaragoza, Spain

[‡]Department of Chemistry, University of Burgos, Burgos, Spain

[§]Department of Chemical Engineering, Qatar University, Doha, Qatar

Supporting Information

ABSTRACT: A study on the viscosity of eight pyridinium based ionic liquids is reported for wide pressure and temperature ranges. Measurements were performed using an electromagnetic moving piston viscometer. Experimental data were fitted to a Tait-like equation demonstrating good correlations, which was used to calculate pressure/viscosity and temperature/viscosity coefficients. The effect of the involved anions and cation on the ionic liquid viscosity was analyzed from a molecular viewpoint using hole theory, quantum chemistry calculations using density functional theory, and classical molecular dynamics simulations. The analysis of the experimental and computational results shows the complex effects controlling viscosity of studied fluids, including strength of ionic pairs, molecular sizes, and mobility and effects rising from the availability and cavity sizes distributions in pyridinium-based ionic liquids.

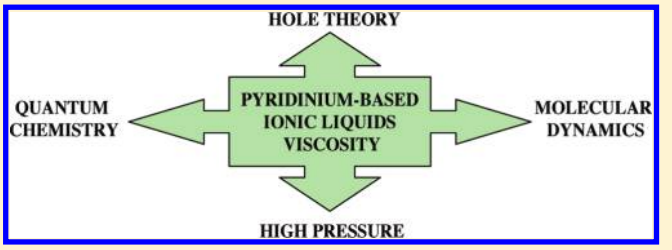

1. INTRODUCTION

The interest on ionic liquids, both in industry and academia, has increased these past few years,[1] which has its roots in the importance of these fluids within the new green chemistry framework[2,3] and their promising properties, and these make them suitable fluids for applications in very different fields such as lubrication, thermal fluids, etc.[4,5] One of the most important properties of ionic liquids is their characteristic of tailor-made fluids, that is to say, fluids that may be designed specifically for each required application through a suitable combination of ions.[6] Nevertheless, although the available studies on different aspects of ionic liquids have grown almost exponentially, the knowledge of the relationships between the molecular level structure and macroscopic properties of these fluids have not been studied in detail.[7−9] The development of accurate and reliable ionic liquid molecular structure−macroscopic fluid properties relationships is, in our opinion, a key step in the advancement of this technology and the use of ionic liquids at an industrial level and not only at a laboratory scale. The use of ionic liquids at an industrial scale requires the knowledge of several thermophysical properties that are used for process design purposes. In a recent review,[10] we showed the state-of-the-art of the most relevant thermophysical properties for ionic liquids, and the main conclusions we inferred were (i) studies are centered on a few ionic liquids and (ii) studies on the pressure effect on these properties are almost absent. Viscosity is one of the most relevant properties required for the characterization of any fluid, because it is related to the molecular mobility,[11] which is governed by intermolecular forces and size and shape effects. Therefore, the accurate description of fluids' viscosity relies on a deep knowledge of molecular level properties. In the case of ionic liquids, although several experimental studies at atmospheric pressure have been conducted, the pressure changes of viscosity have been scarcely studied, and there are not many high pressure viscosity data available;[10] thus, it is a clear problem for the use of ionic liquids at an industrial scale because the knowledge of viscosity at high pressure is required for many proposed applications of ionic liquids, such as lubrication.[12] Moreover, the high viscosity of many ionic liquids in comparison with common organic solvents has been considered as one of the main drawbacks of these fluids because it would hinder many of their possible practical uses for purposes such as mass or heat transfer processes or would make for difficult, and increase the costs of, relevant operations such as fluids pumping or stirring.[5] Therefore, the knowledge of the whole pressure−temperature−viscosity behavior ($P\eta T$) of relevant ionic liquids would allow the most suitable operational conditions for these fluids to be determined. Likewise, considering that it is not clear at present the relationships between the molecular structure and ion−ion interactions with the viscosity, systematic studies for selected families of ionic liquids are required to infer the relevant information required to develop these relationships together with predictive viscosity models for practical purposes.

Received: April 12, 2011
Revised: September 20, 2011
Published: September 22, 2011

dx.doi.org/10.1021/jp203433u | J. Phys. Chem. B 2011, 115, 12499–12513

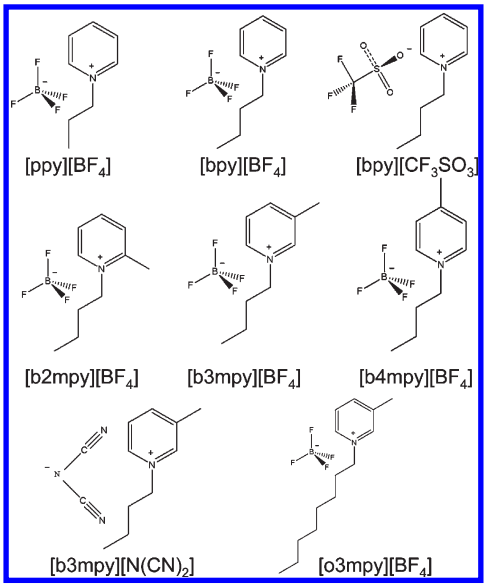

Figure 1. Pyridinium-based ionic liquids studied in this work.

The $P\eta T$ studies available in the open literature for ionic liquids are very scarce, and yet the majority of the available data was devoted to imidazolium based ionic liquids. We also mention the wide study reported by Ahosseini and Scurto,[13] in which $P\eta T$ studies were performed for ionic liquids containing four different cations (imidazolium type) and three different anions, with the viscosity being analyzed in terms of the involved ions' characteristics. Therefore, in this work we report for the first time a $P\eta T$ study on eight selected pyridinium based ionic liquids. Pyridinium based ionic liquids have been proposed for many possible applications such as fuel desulfurization,[14] aromatics extraction,[15] catalysis application,[16] or organic synthesis;[17] therefore, interest in these fluids not only is based on basic science purposes but also has clear practical reasons. Pyridinium-based ionic liquids use to show larger viscosities than their equivalent imidazolium compounds.[18] The structure of the studied compounds is reported in Figure 1, and they were selected to analyze the effect of substituents in the pyridinium cation and the type of anion on the fluid viscosity.

Experimental methods to perform viscosity measurements for ionic liquids have been discussed in the literature and they have been the object of controversy. As Nunes et al.[19] highlighted, there are no primary methods for the measurement of liquids viscosity at this moment; nevertheless, these authors use the term quasiprimary to define those methods working with a physical sounding equation but requiring some type of calibration for some of their parameters. Therefore, methods such as oscillating body, vibrating wire, or quartz crystal method would fit within this quasiprimary category, and thus they were recommended as the primary choice for ionic liquids viscosity measurements;[19,20] nevertheless, we have used in this work an electromagnetic piston viscometer that has showed adequate performance and accuracy for ionic liquids in wide pressure and temperature ranges.[13,21,22]

The theoretical analysis of viscosity for ionic liquids has been developed using several approaches in the literature. Abbot et al.[23,24] used a simple hole theory approach to explain the viscosity of ionic liquids in terms of molecular size. Ahosseini et al.[13] showed that this simple geometric approach does not lead to an adequate explanation of viscosity for imidazolium based fluids; nevertheless, it was tested in this work for the studied pyridinium based ionic liquids. Likewise, as one of the objectives of this work is to understand the molecular basis of the viscosity for the studied pyridinium based ionic liquids two additional computational approaches were considered:

(i) Quantum chemistry calculations were carried out also in this work to analyze the properties of the short-range cation/anion interactions for all of the studied pyridinium based ionic liquids.

(ii) Molecular dynamics simulations to study the molecular level structure of pyridinium based ionic liquids, and its relationship with fluids' viscosity.

Therefore, in this work we have used a wide scope approach to analyze the viscosity of pyridinium based ionic liquids based on fluids molecular level properties.

Table 1. Halide Content of Ionic Liquid Samples Used for Viscosity Measurements

ionic liquid	halide content
[ppy][BF_4]	<0.5%
[bpy][BF_4]	<100 ppm
[bpy][CF_3SO_3]	<100 ppm
[b2mpy][BF_4]	<100 ppm
[b3mpy][BF_4]	<400 ppm
[b4mpy][BF_4]	<550 ppm
[b3mpy][$N(CN)_2$]	<300 ppm
[o3mpy][BF_4]	<200 ppm

2. MATERIALS AND METHODS

Ionic Liquid Samples. Pyridinium-based ionic liquid samples were provided by IoLiTec and Solvent Innovation. Samples were dried for 24 h under a vacuum of 0.05 kPa under stirring and then stored in Schlenk flasks. The water content was measured before any measurement through Karl Fischer titration, and it was lower than 500 ppm for all of the studied mixtures. The halide content of each sample is reported in Table 1. These halide concentrations are low, and they should not have a remarkable effect on the viscosity of the studied ionic liquids. The used samples are colored (from pale yellow to clear brown, depending on the ionic liquid), and procedures for color removal were ruled out as it is not a standard procedure.

Viscosity Measuring Methods. Viscosities (η) were measured using an electromagnetic VINCI Tech. EV1000 viscometer, which is based on a piston electromagnetically driven sensor by Cambridge Viscosity Inc. The scheme of the apparatus is reported in Figure 2. The measurement principle is based on the annular flow around an axially oscillating piston.[13] The system was set up around a measuring sample chamber connected on top and bottom to system lines. A stainless steel piston placed inside the measurement chamber is electromagnetically driven back and forth at a constant force using a magnetic coil, whereas a second coil determines the piston position. The traveling time to complete a cycle is directly related to the sample viscosity. The system allows measurements from 0.02 to 10 000 mPa s by using pistons of different sizes pursuant to the viscosity range to be covered. Measurements can be done in the 253.15 to 473.15 K and up to 100 MPa temperature and pressure ranges, respectively. The sample heating was provided and controlled by an external Julabo LH50 recirculating bath and measured by a built-in platinum resistance probe with ±0.01 K

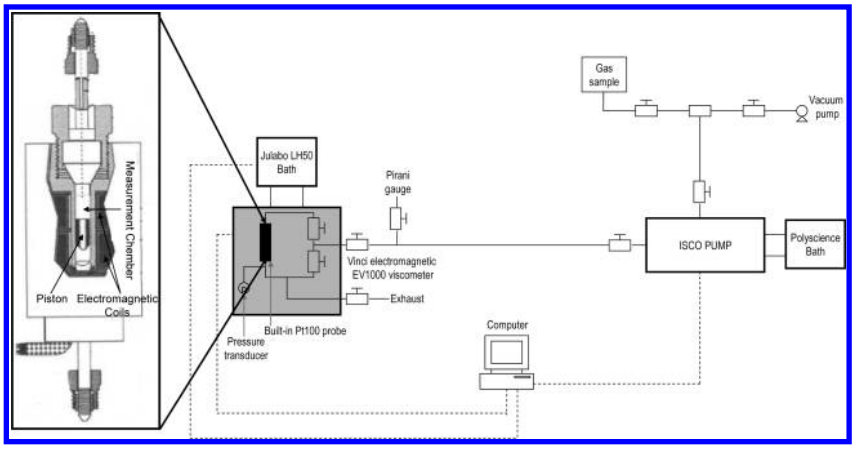

Figure 2. Scheme of the apparatus used for viscosity measurements in this work.

Table 2. Viscosity, η, of the Studied Pyridinium-Based Ionic Liquids in Comparison with Literature Available Data

ionic liquid	T/K	η/ mPa s	ref	method	claimed accuracy	measured water content/ppm
[ppy][BF_4]	293.15	147	this work[a]	electromagnetic	±3%	400
[bpy][BF_4]	293.15	223	this work	electromagnetic	±3%	100
	293.15	223.06	25	rolling ball	±0.3 mPa s	625
	293.15	220.5	26	Ubbelohde	±0.01 mPa s	<500
	293.15	133[b]	27	cone and plate	not stated	not stated
[bpy][CF_3SO_3]	308.15	85.9	this work	electromagnetic	±3%	400
	308.15	76.93	26	Ubbelohde	±0.01 mPa s	<500
[b2mpy][BF_4]	298.15	250	this work	electromagnetic	±3%	450
	298.15	403.3	28	rotational	±1%	<580
	298.15	389.4	29	Ubbelohde	±0.01 mPa s	<500
[b3mpy][BF_4]	293.15	254	this work	electromagnetic	±3%	450
	293.15	246	30	cone and plate	±2%	327
	293.15	246.63	31	Ubbelohde	±0.01 mPa s	<500
[b4mpy][BF_4]	298.15	191	this work	electromagnetic	±3%	425
	298.15	199.9	31	Ubbelohde	±0.01 mPa s	<500
	298.15	202.8	32	Ubbelohde	±1%	560
[b3mpy][$N(CN)_2$]	298.15	32.1	this work	electromagnetic	±3%	300
	298.15	35.2	32	Ubbelohde	±1%	730
	298.15	37.76	33	Ubbelohde	±0.01 mPa s	<500
[o3mpy][BF_4]	293.15	668	this work	electromagnetic	±3%	2300
	293.15	747.4	34	Ubbelohde	±0.01 mPa s	<500

[a] Values obtained in this work for pressure ~0.1 MPa (see Table S1, Supporting Information). [b] Calculated from the reported Vogel−Fulcher−Tamman coefficients.

accuracy. The sample pressure was controlled by an ISCO 100DM syringe pump and measured with a pressure transducer to ±0.1% uncertainty in the full scale. The diameter of the measurement chamber changes with pressure; these changes were corrected with a factory-provided equation.[13]

The whole circuit was degassed before any measurement using an Edwards RV3 rotary vane vacuum pump up down to a pressure around 10 Pa, which is measured with a Pirani Gauge. Previously dried samples were introduced in the apparatus from Schlenk flasks using syringes. Possible bubbles in the measurement chamber were eliminated using a purge feature that rapidly moves the piston. Once the chamber is filled, the temperature is fixed and measurements are performed in an isothermal way with increasing pressures. Every single data point for a fixed temperature and pressure is the average of no less than 200 measurements. The uncertainty of the reported absolute viscosity data in the studied pressure and temperature ranges was estimated to be ±2%.

The apparatus was factory calibrated; viscometer validation was verified using three different procedures. First, standard certified oils such as complex mixtures of hydrocarbons and additives provided by Koehler Inc. were used, which certified viscosity values were measured according to ASTM D2162 (±0.18% viscosity uncertainty or better, depending on the viscosity range). In Figure S1 (Supporting Information) we report a comparison for S6S standard oil between the certified viscosity data and those measured using the electromagnetic viscometer, and adequate agreement may be inferred. Second, measurements using the electromagnetic viscometer for selected

Table 3. Fitting Parameters Obtained from the Fit of Experimental $P\eta T$ Data (Table S1, Supporting Information) to Tait Equation (eqs 1 and 2)

	[ppy][BF_4]	[bpy][BF_4]	[bpy][CF_3SO_3]	[b2mpy][BF_4]
A/ mPa s	0.03946	0.08948	0.20153	0.01125
B/K	1104.26	903.16	684.74	1526.46
C/K	158.77	177.72	195.08	145.64
D	2.8004	3.3593	19.9977	24.5648
E_0/MPa	−3617.79	−2278.98	−2281.00	−5000.00
E_1/MPa K^{-1}	23.035	13.832	10.238	22.288
E_2/MPa K^{-2}	−0.03362	−0.01744	0.00959	0.00309
σ/%	1.81	1.26	2.24	2.14

	[b3mpy][BF_4]	[b4mpy][BF_4]	[b3mpy][$N(CN)_2$]	[o3mpy][BF_4]
A/ mPa s	0.06496	0.1107	0.16341	0.0147
B/K	964.50	811.36	681.49	1500.00
C/K	176.57	189.21	169.05	153.76
D	12.2330	19.3014	4.3317	3.6595
E_0/MPa	5000.00	−4602.51	−1000.00	4437.21
E_1/MPa K^{-1}	−35.759	25.673	2.965	−28.944
E_2/MPa K^{-2}	0.07441	−0.01823	0.00748	0.04986
σ/%	1.08	1.52	1.30	5.15

ionic liquids were compared with those performed in our laboratory using an Anton Paar AMV200 rolling ball viscometer (±3% viscosity uncertainty, ±0.01 K), at atmospheric pressure, Figure S2 (Supporting Information). Third, experimental data measured with electromagnetic viscometer at atmospheric pressure were compared with available literature viscosity data. Values at 298.15 K are reported in Table 2 and refs 25−34, and a comparison as a function of temperature is reported in Figure S3 (Supporting Information). A good consistency is obtained for most of the studied ionic liquids between the values obtained in this work with the electromagnetic viscometer and the literature data obtained with different experimental methods. Discrepancies are obtained especially for [b2mpy][BF_4], for which the values reported in this work are remarkably lower than those obtained in the literature. Nevertheless, remarkable discrepancies between different literature sources are common for many ionic liquids as we reported in a recent review;[10] the origin of these differences is not fully clarified, and it can not always be assigned to the purity of the used samples. Moreover, the problems associated with the use of some experimental techniques for the measurement of ionic liquids viscosity reported in the literature,[19] and the true accuracy of many nonprimary viscosity measurement methods[20] could be the origin of some of these discrepancies. Therefore, the three used procedures allow the measured viscosity data reported in this work to be validated using the reported electromagnetic viscometer. To our knowledge, there are no available data for high pressure conditions for any of the studied ionic liquids reported in this work, and thus, further comparisons on the pressure effect for the viscosity of the studied ionic liquids are not possible. $P\eta T$ data for the eight studied pyridinium-based ionic liquids are reported in Table S1 (Supporting Information), and measurements were carried out in the ∼0.1 to 65 MPa pressure range and up to 333.15 K for temperatures above the melting temperature of each ionic liquid. Since there are no available reported data at high pressures for any of the studied ionic liquids reported in this work, further comparisons on the pressure effect for the viscosity of the studied ionic liquids are not possible.

Experimental $P\eta T$ data were fitted to the Tait equation over the whole pressure/temperature ranges[35]

$$\eta = A \exp\left(\frac{B}{T - C}\right) \exp\left(D \ln\left(\frac{P + E}{0.1\ \text{MPa} + E}\right)\right) \quad (1)$$

where E parameter is temperature dependent

$$E = E_0 + E_1 T + E_2 T^2 \quad (2)$$

the parameters A, B, C, D, E_0, E_1, and E_2 were fitted by a least−squares procedure. Fitting quality was quantified using eq 3.

$$\sigma = 100 \sqrt{\frac{1}{n} \sum_{i=1}^{n} \left(\frac{\eta_i^{\text{exp}} - \eta_i^{\text{cal}}}{\eta_i^{\text{exp}}}\right)^2} \quad (3)$$

Fitting parameters are reported in Table 3. The pressure viscosity (α_η) and temperature viscosity (β_η) coefficients were calculated according to eqs 4 and 5 and reported in Table S2 (Supporting Information)

$$\alpha_\eta = \left(\frac{1}{\eta}\right)\left(\frac{\partial \eta}{\partial P}\right)_T = \frac{D}{P + E} \quad (4)$$

$$\beta_\eta = -\left(\frac{1}{\eta}\right)\left(\frac{\partial \eta}{\partial T}\right)_P = \eta\left(\frac{-B}{(T - C)^2}\right) + \eta D(E_1 + 2E_2 T)\frac{0.1\ \text{MPa} - P}{(0.1\ \text{MPa} + E)(P + E)} \quad (5)$$

Quantum Chemistry Calculations. Density functional theory (DFT) was used for all of the calculations to analyze the

properties of involved ionic pairs for the studied pyridinium based ionic liquids. Calculations were carried out with the Gaussian 03 package[36] using the Becke gradient corrected exchange functional[37] and Lee−Yang−Parr correlation functional[38] with the three parameter (B3LYP)[39] method. The 6-311++g** basis set was used in this work. Atomic charges were calculated to fit the electrostatic potential[40] according to the Merz−Singh−Kollman (MK)[41] scheme. Interaction energies for the ionic pairs, ΔE, were calculated as the differences among the pair and sum of corresponding cation and anion energies at the same theoretical level, with basis set superposition error (BSSE) corrected through the counterpoise procedure.[42] Moreover, atom in molecule (AIM) calculations[43] were carried out using the AIM2000 program[44] to get deeper insight into anion/cation interactions.

Molecular Dynamics Simulations. Classical molecular dynamics simulations were carried out using the TINKER molecular modeling package.[45] All simulations were performed in the NPT ensemble; the Nosé−Hoover method[46] was used to control the temperature and pressure of the simulation system. The motion equations were solved using the Verlet Leapfrog integration algorithm.[47] Long-range electrostatic interactions were treated with the smooth particle mesh Ewald method.[48] The simulated systems consist of cubic boxes, containing 125 ion pairs for all of the studied ionic liquids, to which periodic boundary conditions were applied in three directions to simulate an infinite system. The simulations were performed using a cutoff radius of 10 Å. Initial boxes were generated using the PACKMOL program,[49] and according to this approach, the ions are packed within spatial regions in such a way that atoms from different ions keep a safe pairwise distance according to different constraints. The initial cell volume was chosen to be 0.60 g cm^{-3} for all of the simulations to avoid any effect rising from possible initial configurations built close to the experimental densities. The equilibration procedure is remarkably important for simulations involving ionic liquids. The dynamics of ionic liquids is very slow;[50] therefore, long simulation times are needed for computing the properties of these fluids. Procedures for equilibration and production have to be designed carefully to avoid the presence of local minima in these slow simulations. Thus, with this purpose, initial boxes were minimized according to the MINIMIZE program in the TINKER package to a 0.01 kcal mol^{-1} $Å^{-1}$ rms gradient. Therefore, several heating and quenching steps in the NVT ensemble up to 500 K were performed after which a 100 ps NVT equilibration molecular dynamics simulation was run at the studied temperature. Finally, from the output NVT simulation configuration, a run of 10 ns (time step 1 fs) in the NPT ensemble at the studied pressure and temperature was run, from which the first 5 ns were used to ensure equilibration (checked through constant energy) and the remaining 5 ns for data collection. Considering the low self-diffusion coefficients (high viscosities) of the studied fluids, simulation results may be dependent on the initial conditions used for the simulations. Therefore, several uncorrelated initial boxes were built for each ionic liquid, and simulations were performed at 303 K and 0.1 MPa for 10 ns using the described procedure. The final results of the simulations were analyzed through a comparison of radial distribution functions, interaction energies and simulated densities; no remarkable differences were found between the simulations using different initial conditions, and thus, we may conclude that the reported method should lead to representative results on the molecular level structure and properties of the studied fluids.

Pyridinium based ionic liquids were described according to the so-called optimized potential for liquid simulations (all atom version) OPLS−AA, eq 6[51]

$$E = \sum_{\text{bonds}} k_r(r - r_{eq})^2 + \sum_{\text{angles}} k_\theta(\theta - \theta_{eq})^2 + \sum_{\text{torsions}} \frac{V_1}{2}[1 + \cos(\phi + f_1)] + \frac{V_2}{2}[1 - \cos(2\phi + f_2)] + \frac{V_3}{2}[1 + \cos(3\phi + f_3)] + \sum_i \sum_j \left\{ 4\varepsilon_{ij}\left[\left(\frac{\sigma_{ij}}{r_{ij}}\right)^{12} - \left(\frac{\sigma_{ij}}{r_{ij}}\right)^{6}\right] + \frac{q_i q_j e^2}{r_{ij}} \right\} \quad (6)$$

Where the first three terms in eq 6 represent the bonded interactions: bonds, angles, and torsions. The nonbonded interactions include van der Waals (Lennard-Jones 6−12 form) and Coulombic interactions of atom-centered point charges. Nonbonded interactions were calculated for the atoms in different molecules or in the same molecule separated by more than three bonds. The nonbonded 1−4 interactions are reduced by a 0.5 scale factor. The Lennard-Jones parameters for unlike atoms were obtained from the Lorentz−Berthelot combining rule. Forcefield parameters for all studied cations and anions are reported in Table S3 (Supporting Information). Parameters were obtained from Maggin et al.[52] and Canongia-Lopes et al.,[53] van der Waals parameters for pyridinium rings were slightly modified to reproduce experimental density data, and torsional parameters were transformed to OPLS-AA three terms torsional form when required. Atomic charges for molecular dynamics simulations cannot unambiguously be determined because they are not experimentally available, and thus a large number of methods have been proposed. MK charges calculated as reported in the previous section were used in this work, Table S3 (Supporting Information). Molecular dynamic simulations were performed for [bpy][BF_4], [b3mpy][BF_4], [b3mpy][$N(CN)_2$], and [o3mpy][BF_4] to analyze the main structural features of the cations and anions studied in this work.

3. RESULTS AND DISCUSSION

Experimental $P\eta T$ reported in Table S1 (Supporting Information) were successfully correlated with the Tait equation as the low deviations reported in Table 3. The largest deviations in the correlation were obtained for [o3mpy][BF_4], the most viscous fluid studied in this work. Nevertheless, obtained deviations for the correlated data are in the range of previously reported high pressure viscosity data for common imidazolium based ionic liquids using correlating equations with a similar number of fitting parameters.[13]

The selected studied ionic liquids allow us to analyze the effect of anions and cations on the fluids viscosity. As this is the first available study on the pressure effect on pyridinium-based ionic liquids viscosity, we will discuss temperature effects on fluids' viscosity, using a molecular level approach that would allow us to increase the available literature information,[26,29,31,33] but the

analysis will be also extended to the behavior under pressure at the end of this work.

3.1. Analysis of Viscosity According to Hole Theory. The hole theory approach used by Abbot et al.[23,24] allows an initial analysis of the viscosity as a function of the properties of the involved anions and cations for the studied fluids. This simple model assumes that ionic liquids contain empty spaces because of thermal fluctuations of local density, and thus, fluid viscosity is related to the mobility of ions toward empty holes of adequate size. The probability, P, of finding a hole of radius r may be calculated using eq 7

$$Pdr = \frac{16}{15\sqrt{\pi}} a^{7/2} r^6 e^{-ar^2} dr \quad (7)$$

Where a parameter may be calculated from the surface tension, γ, of the fluid, eq 8

$$a = 4\pi\frac{\gamma}{T} \quad (8)$$

Therefore, integrating eq 7 from R^* to ∞ leads to the probability of finding a hole of suitable dimensions to which ions may move, and thus, it may be inferred how difficult it is for an ion to find a hole of adequate size and, thus, to relate this effect with viscosity. Abbot et al.[23,24] proposed to use in the calculations of probability the average ion radius ($R^* = R_\pm = (R_+R_-)^{1/2}$). We have tested this approach in this work, and it lead to very large deviations with experimental viscosity data. Therefore, we defined an effective ionic liquid radius, R^*, which was obtained applying the hole theory to experimental viscosity data at 0.1 MPa and fitting R^*, considered a temperature dependent parameter. Results of the application of hole theory for the eight studied pyridinium based ionic liquids at 313.15 K and pressures around 0.1 MPa are reported in Table 4 and Figure 3, whereas the application in the 283.15−333.15 K range are shown in Figure 4. Deviations between experimental and predicted viscosity data are acceptably low considering the simplicity of the approach (absolute percentage deviations lower than 7%). Likewise, there is a clear relationship between the probability of finding a hole of adequate size, $P(r > R^*)$, and the viscosity: the lower $P(r > R^*)$, the larger the viscosity. Moreover, this relationship is clearly linear as results reported in Figure 3 for isothermal conditions show, and it is maintained in the whole studied temperature range, Figure 4a, for the studied ionic liquids. Therefore, it may be concluded that the availability of cavities of adequate size must play a relevant role for the fluidity of pyridinium based ionic liquids. Nevertheless, a question rises from this methodology: which is the true meaning of the R^* parameter? The values of this parameter are reported in Figure 4b for the eight pyridinium based ionic liquids as a function of temperature, showing that R^* decreases with the temperature, with the larger R^*, the lower the fluidity. Anion and cation radii, R_+ and R_-, were calculated from the Connolly solvent excluded volume for each ion, from structures optimized through quantum chemistry methods at B3LYP/6-311++g** theoretical level for independent anions and cations, supposing spherical shape, and thus, $R_\pm = (R_+R_-)^{1/2}$ were calculated from these values and compared with R^*, Figure 5. R^* values are close to $R_\pm$ ones, with deviations lower than 5%, except for [b3mpy][N(CN)$_2$] and [o3mpy][BF$_4$]. R^* is 21% lower than $R_\pm$ for [b3mpy][N(CN)$_2$]. This compound is the less viscous of the studied ionic liquids, and it has a large surface tension (49.49 mN m^{-1} at 313.15 K).[33] Likewise, R^* is 16% larger than $R_\pm$ for [o3mpy][BF$_4$], which has low surface tension (35.02 mN m^{-1} at 313.15 K).[34] Therefore, the presence of these two outlying points in Figure 5 shows that the hole theory leads to an incomplete description of the these fluids.

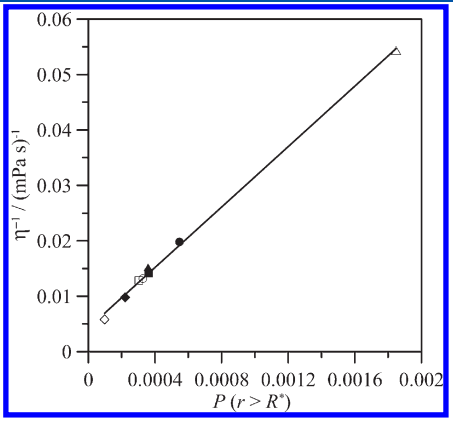

Figure 3. Relationship between experimental fluidity, η^{-1} (Table S1, Supporting Information), and probability of finding a hole of radius larger than effective radius, $P(r > R^*)$, for the studied pyridinium based ionic liquids at 313.15 K and a pressure around 0.1 MPa. Symbols: (●) [ppy][BF$_4$]; (■) [bpy][BF$_4$]; (▲) [bpy][CF$_3$SO$_3$]; (◆) [b2mpy][BF$_4$]; (○) [b3mpy][BF$_4$]; (□) [b4mpy][BF$_4$]; (△) [b3mpy][N(CN)$_2$]; and (◇) [o3mpy][BF$_4$]. Continuous line shows linear fit.

Table 4. Results of the Application of Hole Theory for the Prediction of Viscosity Data for the Reported Pyridinium Based Ionic Liquids at 313.15 K and Atmospheric Pressure[a]

ionic liquid	$10^4 \times P(r > R^*)$	R^*/Å	$\eta_{ca.\ 1}$/mPa s	η_{exp}/mPa s	percentage deviation
[ppy][BF$_4$]	5.47	2.40	51.7	50.5	−2.3
[bpy][BF$_4$]	3.62	2.60	68.7	70.5	2.5
[bpy][CF$_3$SO$_3$]	3.59	2.93	62.2	66.7	6.8
[b2mpy][BF$_4$]	2.21	2.72	105	102	−3.0
[b3mpy][BF$_4$]	3.27	2.68	73.0	75.9	3.9
[b4mpy][BF$_4$]	3.03	2.69	79.9	77.8	−2.7
[b3mpy][N(CN)$_2$]	18.48	2.10	19.7	18.4	−6.8
[o3mpy][BF$_4$]	0.98	3.27	178	172	−3.0

[a] $P(r > R^*)$ stands for the probability of finding a hole of radius, r, larger than the effective radius, R^*, of the ionic liquid, calculated according to eqs 6 and 7; η_{cal} stands for the dynamic viscosity calculated using hole theory; η_{exp} stands for the experimental dynamic viscosity data measured in this work at pressures around 0.1 MPa (Table S1, Supporting Information); percentage deviation stands for the deviation between experimental and calculated dynamic viscosity.

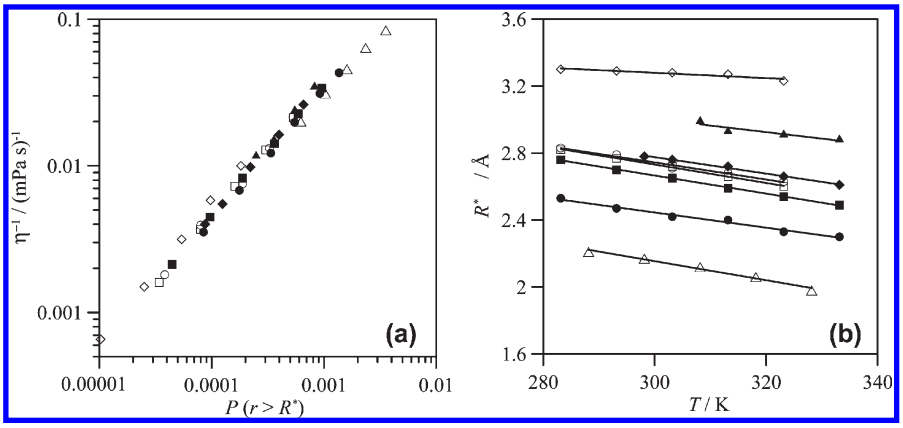

Figure 4. (a) Relationship between experimental fluidity, η^{-1} (Table S1, Supporting Information), and probability of finding a hole of radius larger than effective radius, $P(r > R^*)$, and (b) effective radii, R^*, as a function of temperature, for the studied pyridinium based ionic liquids in the 283.15−333.15 K temperature range and pressure around 0.1 MPa. Symbols as in Figure 3. Continuous lines in panel b shows linear fits.

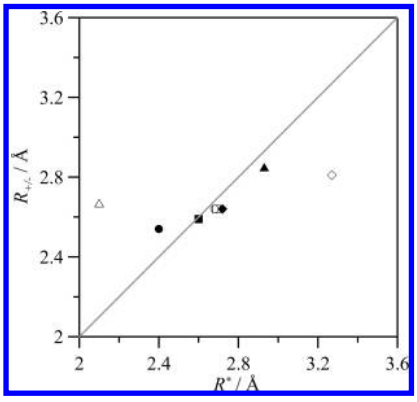

Figure 5. Relationship between effective radii, R^*, and average ionic radii, $R_{\pm}$, for the studied pyridinium based ionic liquids at 313.15 K and pressure around 0.1 MPa. Symbols: (●) [ppy][BF_4]; (■) [bpy][BF_4]; (▲) [bpy][CF_3SO_3]; (◆) [b2mpy][BF_4]; (○) [b3mpy][BF_4]; (□) [b4mpy][BF_4]; (Δ) [b3mpy][$N(CN)_2$]; and (◇) [o3mpy][BF_4]. Continuous gray line shows line of equal values ($R^* = R_{\pm}$).

3.2. Analysis of Viscosity According to Quantum Chemistry Calculations. Suzuki et al.[54] have recently reported that at least three main factors develop important roles in the magnitude of self-diffusion coefficients, and thus of viscosity, for ionic liquids: (i) size, (ii) shape, and (iii) interaction energies for anion−cation pairs. These factors can be analyzed through quantum chemistry methods as proposed in this work. The analysis of anion/cation interactions performed through gas phase quantum chemistry methods is obviously a simplified approach because the properties of these ionic pairs would change on going to liquid phase because of the presence of neighbor ions. Nevertheless, the aforementioned factors, together with short-range interactions, can be analyzed through these methods at least in a qualitative way to infer the main trends that govern viscosity from the viewpoint of the molecular properties of the involved ions.

Interaction energies, ΔE, for optimized structures of anion−cation pairs (Figure S4, Supporting Information) are reported in Table 5. The studied cations may adopt several conformations near to room temperature, but this fact was ignored in this work and only the lower energy conformers were analyzed in a first approach. Optimized structures for ionic pairs reported in Figure S4 (Supporting Information) show that studied anions appears close to the pyridinium ring for all of the studied cations, in particular close to the nitrogen atom. For BF_4^- containing ionic liquids, the interaction of the anion with the pyridinium cations is developed through multiple contacts with the hydrogen of the pyridinium ring and those in the head (close to pyridinium nitrogen) of the alkylic chains. The anion−cation interaction is developed mainly through purely electrostatic interactions (Coulombic type); nevertheless, the interactions between the anion and C−H hydrogens may be classified as hydrogen bonds as interatomic distances, angles, and AIM analysis show, and thus, they should also develop a relevant role in the ionic pair stability and properties. According to the AIM approach, two main criteria must be fulfilled to define a true hydrogen bonding: (i) a bond path between two atoms, with the existence of a bond critical point, BCP, in the middle of the path and (ii) the electron density at BCP, ρ_{BCP}, and the laplacian of that electron density, $\nabla^2\rho_{BCP}$, must be within the 0.002−0.035 and 0.024−0.139 ranges, respectively, both in atomic units.[55,56] We report in Figure 6 AIM results for [b3mpy]BF_4 ionic liquid. Specially for the C−H···F interaction, interatomic distances and angles fall within the hydrogen bonding range, leading to moderate hydrogen bonding specially for positions 1 and 6. These results are in agreement with those reported by Sun et al.[57] for [bpy][BF_4]. This is confirmed by the AIM analysis reported in Figure 6b,

Table 5. Counterpoise Corrected Interaction Energy, ΔE, Connolly Solvent Excluded Volume, CSEV, and Ovality for Anion−Cation Pairs in the Gas Phase Calculated at the B3LYP/6-311++g Theoretical Level[a]**

ionic liquid	ΔE/kJ mol^{-1}	CSEV/Å^3	ovality
[ppy][BF_4]	−330.16	164.48	1.3189
[bpy][BF_4]	−323.67	181.75	1.3526
[bpy][CF_3SO_3]	−302.13	218.29	1.3846
[b2mpy][BF_4]	−316.23	202.83	1.3170
[b3mpy][BF_4]	−319.49	203.47	1.3378
[b4mpy][BF_4]	−313.42	203.99	1.3369
[b3mpy][$N(CN)_2$]	−308.53	210.25	1.3254
[o3mpy][BF_4]	−269.45	272.58	1.4729

[a] All values calculated for structures reported in Figure S4 (Supporting Information).

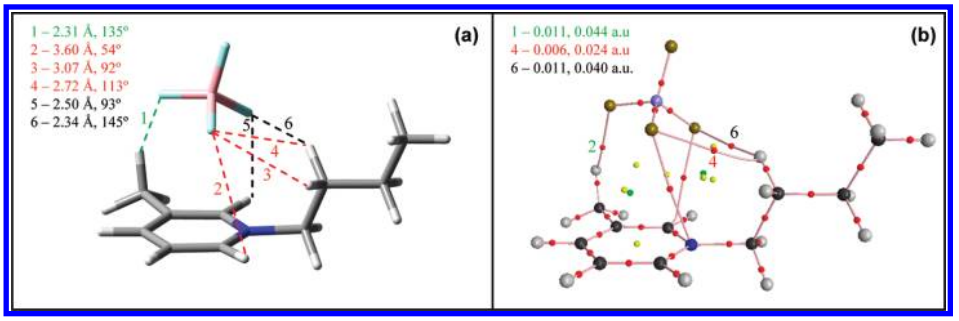

Figure 6. Properties of the [b3mpy][BF_4] ionic pair calculated at B3LYP/6-311++g** theoretical level. In panel a we report several relevant C−H···F distances and angles and in panel b the AIM analysis of the pair showing bond critical points (BCP, red circles), ring critical points (yellow circles) and cage critical points (green circles), including data for electron density and laplacian of electron density at relevant BCPs (in this order). In panel b we report only bond paths (pink lines) but not ring and cage paths for the sake of visibility.

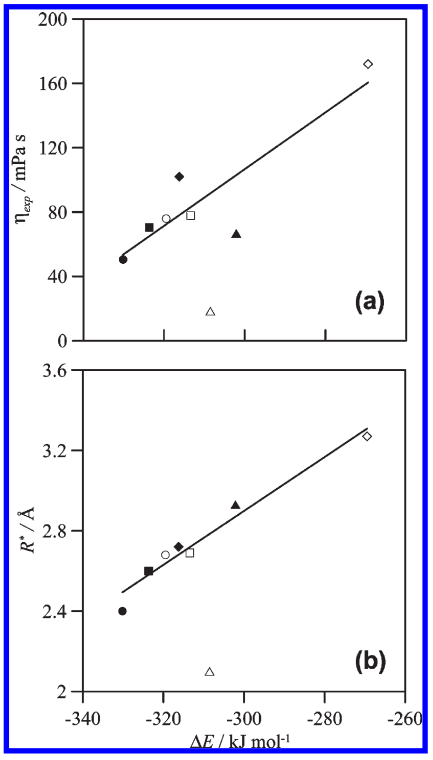

Figure 7. Relationship between counterpoise corrected anion−cation interaction energy, ΔE, calculated in gas phase at B3LYP/6-311++g** theoretical level and (a) experimental viscosity, η_{exp}, and (b) effective radii, R^*, for the studied pyridinium based ionic liquids at 313.15 K and pressure around 0.1 MPa. Symbols: (●) [ppy][BF_4]; (■) [bpy][BF_4]; (▲) [bpy][CF_3SO_3]; (◆) [b2mpy][BF_4]; (○) [b3mpy][BF_4]; (□) [b4mpy][BF_4]; (Δ) [b3mpy][$N(CN)_2$]; and (◇) [o3mpy][BF_4]. Continuous lines show linear fits of data excluding values for [b3mpy][$N(CN)_2$].

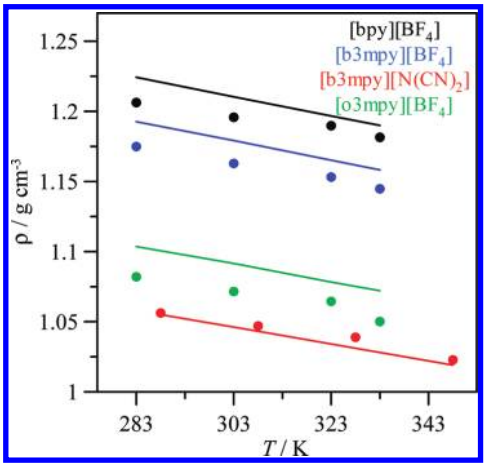

Figure 8. Experimental and simulated densities, ρ, for pyridinium based ionic liquids at 0.1 MPa. Simulated densities are obtained from molecular dynamics simulations with forcefield parameters reported in Table S3 (Supporting Information). Symbols: (continuous lines) experimental values and (circles) simulated values. Experimental values are obtained from Bandrés et al.[26,31,33,34]

which show values of ρ_{BCP}, and $\nabla^2\rho_{BCP}$ close to the lower limit of hydrogen bonding. Nevertheless, in spite of the moderate to weak strength of the C−H---F hydrogen bonds the AIM analysis shows a complex and effective interaction between anion and cation with the presence of ring and cage critical points. Analogous results are obtained for the remaining studied pyridinium ionic liquids.

Results plotted in Figure 7 show a linear relationship between ΔE, R^* (obtained in the previous section from the hole application of the hole theory), and viscosity, with the exception of data for [b3mpy][$N(CN)_2$]: the larger the anion−cation interaction (more negative ΔE), the lower the R^* and viscosity values. This result is in certain manner surprising because we could have expected that stronger interionic electrostatic forces should lead to a certain retardation in the movement of the ion pairs toward the available holes, and thus, to an increase in the viscosity.[23] Therefore, size and shape should develop a relevant role in fluids' viscosity, as reported in the previous section according to the hole theory. We have reported in Table 5 two remarkable geometric parameters: (i) Connolly solvent excluded volume (CSEV, to show ionic pairs sizes) and (ii) ovality (deviation from the spherical shape, defined as the difference between the largest and smallest outside diameter on a cross-section, to show ionic pairs shapes), these factors were calculated for optimized structures reported in Figure S4 (Supporting Information). Nevertheless, although it has been reported in the literature that lower ovality values (that is to say, shapes close to spherical one) tend to increase viscosity,[58] we did not come to any clear conclusion about the relationship if any between CSEV, ovality, and viscosity for pyridinium based ionic liquids.

Table 6. Simulated Enthalpies of Vaporization, ΔH_{vap}, for Pyridinium-Based Ionic Liquids at 298 K/0.1 MPa[a]

	ΔE_{Coul}/kJ mol^{-1}	ΔE_{VdW} /kJ mol^{-1}	ΔE_{Geom}/kJ mol^{-1}	ΔH_{vap}/kJ mol^{-1}	ΔH_{vap}(exp)/kJ mol^{-1}
[bpy]BF_4	113.1	70.6	4.4	190.6 ± 7.6	167 ± 2[b]
[b3mpy]BF_4	111.7	70.7	5.1	190.0 ± 7.1	
[b3mpy]$N(CN)_2$	103.5	69.7	4.8	180.5 ± 6.8	162.1 ± 4[c]
[o3mpy]BF_4	117.6	78.0	5.5	203.6 ± 7.4	

[a] We report coulombic (ΔE_{Coul}), van der Waals (ΔE_{VdW}), and geometric ($\Delta E_{Geom} = \Delta E_{bond} + \Delta E_{angle} + \Delta E_{dihedral} + \Delta E_{improper}$) contributions to the total enthalpies of vaporization. $\Delta E = E_{GAS} - E_{LIQUID}$. Gas properties are calculated for a single ionic pair at the same temperature and pressure. ΔE_{Coul} and ΔE_{VdW} include both intra- and intermolecular contributions. We report also experimental enthalpies of vaporization, ΔH_{vap}(exp), obtained from the literature. [b] Reference 60. [c] Reference 61.

3.3. Analysis of Viscosity According to Molecular Dynamic Simulations. Molecular dynamic simulations were performed for [bpy][BF_4], [b3mpy][BF_4], [b3mpy][$N(CN)_2$], and [o3mpy][BF_4] ionic liquids at four temperatures (isobaric conditions) and four pressures (isothermal conditions), that is to say, eight simulations were performed for each fluid to analyze pressure and temperature effects, and ionic liquids were selected to infer the main structural features for pyridinium based ionic liquids. Viscosity of pyridinium based ionic liquids have not been studied and systematically analyzed, in wide pressure−temperature ranges, through molecular dynamics simulations. Moreover, this study extends previous simulations for pyridinium based ionic liquids reported by Cadena et al.[52] (based on pyridinium ionic liquids with Tf_2N^- anions), Canongia-Lopes et al.[53] (in which a forcefield parametrization was proposed), and Sun et al.[57] (which was limited to [bpy][BF_4] ionic liquid without analyzing pressure or temperature effect).

The simulations performance was analyzed through comparison of predicted density with available experimental data, Figure 8. Reported results show deviations between experimental and simulated density lower than 2% for all the studied ionic liquids, with the average percentage deviations being +0.99, +1.27, −0.40, and +1.78% for [bpy][BF_4], [b3mpy][BF_4], [b3mpy][$N(CN)_2$], and [o3mpy][BF_4], respectively. These deviations show the high reliability and accuracy of the proposed model for the description of molecular-level behavior that lead to an adequate description of macroscopic properties. Nevertheless, we should remark that density is a mean-field property, and thus, Maginn[8] recommended the comparison with other properties more sensitive to forcefield parametrization, such as vaporization enthalpy, for model validation. Vaporization enthalpy, ΔH_{vap}, was calculated according to eq 9

$$\Delta H^{vap} = (U^{ion\,pair} - U^{liq}) + RT \quad (9)$$

where U stands for the average internal energy of ion pair (assuming that it mimics the ideal gas phase) and liquid phase. As the work by Ködermann et al.[59] has shown, van der Waals and electrostatic (Coulombic) energy terms contribute in a different way to the total energy of vaporization, and thus, it is useful to analyze both contributions separately, Table 6. Predicted ΔH_{vap} values are larger that experimental data,[60,61] 14% and 11% for [bpy][BF_4] and [b3mpy][$N(CN)_2$] ionic liquids, respectively. These deviations are reasonable, and thus, forcefield parametrization may be considered as satisfactory, and although Borodin[62] reported that more accurate predictions could be obtained using polarizable forcefields, this possibility was not studied in this work. Nevertheless, Borodin[63] analyzed the relationship between the accuracies of predictions for enthalpies of vaporization and dynamic properties, including viscosity, showing that an overestimation of around 10 kJ mol^{-1} for ΔH_{vap} leaded to an overestimation of viscosity by a factor of 2. Therefore, we may expect that the forcefield parametrization used in this work leads to an overestimation of viscosity and thus to an underestimation of self-diffusion coefficients for the studied pyridinium based ionic liquids. Nevertheless, our main interest is to analyze the molecular factors controlling the viscosity of the studied fluids, and thus, this can be done with the current parametrization in spite of the more viscous character predicted by the simulations in comparison with the experimental data.

The different contributions to the total ΔH_{vap} predicted by molecular dynamics are also reported in Table 6, and for all OF the studied pyridinium-based ionic liquids electrostatic contributions is larger than van der Waals ones. Both contributions are larger for pyridinium based ionic liquids than for imidazolium based ones,[59] especially for the electrostatic term, which is in agreement with the larger experimental ΔH_{vap} for imidazolium ionic liquids. We should remark that the electrostatic term for ionic liquids containing $[BF_4]^-$ anion remains almost constant, independently of the considered cation, and being larger than electrostatic term for $[N(CN)_2]^-$. Moreover, the van der Waals term increases with increasing chain lengths, although in a weaker way than for imidazolium ionic liquids. van der Waals contribution to ΔH_{vap} for 1-alkyl-3-methylimidazolium bis-(trifluoromethylsulfonyl)imide increases 40% on going from butyl to octyl chains, whereas on going from [b3mpy][BF_4] to [o3py][BF_4], the van der Waals term increases only 11%. The ordering of experimental viscosity is [o3mpy][BF_4] > [bpy][BF_4] ≈ [b3mpy][BF_4] > [b3mpy][$N(CN)_2$], which is in agreement with ΔH_{vap} reported in Table 6, and increases/decreases of around 10−15 kJ mol^{-1} lead to large viscosity variations.

Borodin[64] reported several correlations between dynamic properties of ionic liquids, enthalpies of vaporization and cation−anion binding energies. A similar analysis was performed in Figure 7 from calculated gas-phase binding energies, as analyzed in the previous section. Therefore, we explored the possible relationship between the intermolecular (interionic) interaction energy, E_{inter}, obtained from liquid phase molecular dynamics simulations and experimental viscosity data for the studied ionic liquids. E_{inter} was calculated from eq 10, where each term contains both van der Waals and electrostatic contributions.

$$E_{inter} = E_{anion-cation} + E_{anion-anion} + E_{cation-cation} \quad (10)$$

Calculated E_{inter} values are reported in Figure 9 as a function of pressure and temperature. Results reported in Figure 9 show that for a fixed ionic liquid larger E_{inter} (in absolute value) lead to larger viscosity, for the four studied ionic liquids. E_{inter} decreases with temperature and increases with pressure in a similar way as

experimental viscosity data evolves. Nevertheless, E_{inter} values are very similar for the four studied ionic liquids; for example, at 303 K/0.1 MPa, E_{inter} ranges from −502.51 to −508.46 kcal mol^{-1}, whereas viscosity values are in the 21.9−317 mPa s range. Moreover, the ordering of E_{inter} is not in agreement with the ordering of experimental viscosity, for example, at 303 K/0.1 MPa, E_{inter} values are (in absolute value) [b3mpy][N(CN)$_2$] < [b3mpy][BF$_4$] < [o3mpy][BF$_4$] < [bpy][BF$_4$], whereas viscosity data are [b3mpy][N(CN)$_2$] < [b3mpy][BF$_4$] ≈ [bpy][BF$_4$] < [o3mpy][BF$_4$]. Therefore, fluidity of the studied ionic liquids should be determined not only by the strength of the cation−anion interaction, which develops a relevant role, but also factors rising from the sizes and shapes of the corresponding ionic pairs. Some authors have showed that fluidity in ionic liquids is characterized by the presence of ion pairing in these fluids, and thus, ions move in pairs, or clusters, instead of free ions.[52]

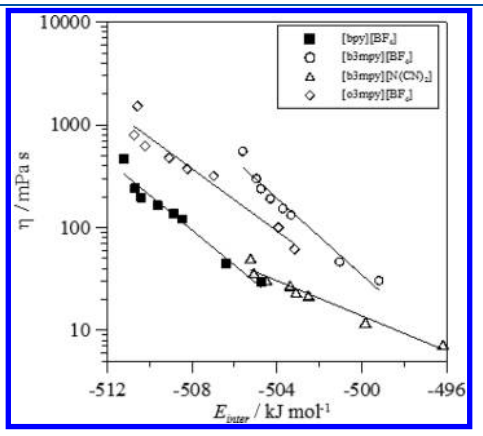

Figure 9. Relationship between experimental viscosity, η, and calculated intermolecular (interionic) interaction energy, E_{inter}.

Molecular dynamics simulations allow inferring the main characteristics of the structural features at the molecular level for the studied pyridinium-based ionic liquids. Radial distribution, RDFs, functions are reported in Figures 10 and 11. Results obtained in this work for [bpy][BF4] are in good agreement with those recently reported by Sun et al.[57] RDFs are characteristic of highly ordered fluids, with a remarkable structuring for large distances, as may be inferred from the maxima and minima obtained for the four studied ionic liquids, Figure 10. Anion−cation RDFs are characterized by a first strong and sharp peak at 4.9 Å for BF_4^- containing ionic liquids, and the position of this peak does not change on going from [bpy][BF$_4$] to [b3mpy][BF$_4$] to [o3mpy][BF$_4$], that is to say, it is not affected by the cation (only the intensity of the peak increases for the bigger cation). Nevertheless, the anion has a remarkable effect on anion−cation RDFs. The first peak for [b3mpy][N(CN)$_2$] shifts toward lower distances (maximum at 4.2 Å), and it is less intense in comparison with BF_4^- containing ionic liquids. Moreover, anion−cation RDFs for [b3mpy][N(CN)$_2$] are less structured. The second peak appearing at 11 Å is clearly less intense than for the remaining fluids, and thus, we may infer that long-range interactions are weaker in [b3mpy][N(CN)$_2$], and thus, this fluid is less structured than BF_4^- containing ionic liquids. This would be in

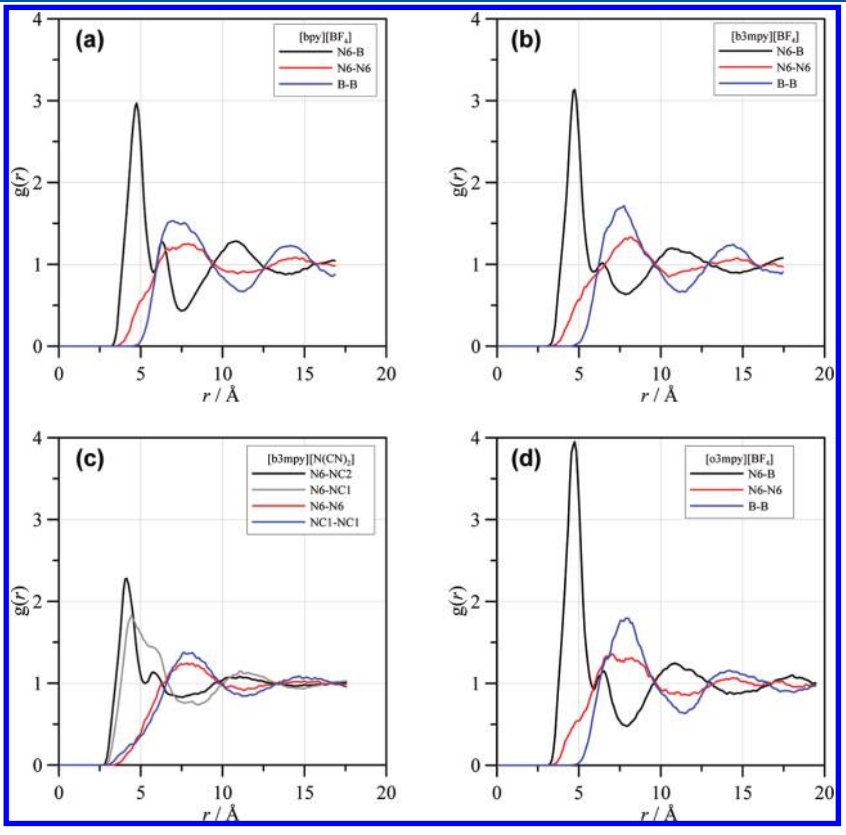

Figure 10. Radial distribution functions, g(r), for pyridinium based ionic liquids at 333 K and 0.1 MPa. Atom code as in Table S3 (Supporting Information); N6 (pyridinium ring nitrogen), B (BF_4^-), and NC1/NC2 (central, NC1, and terminal, NC2, nitrogens in dycianamide) are selected to represent cations and anions, respectively.

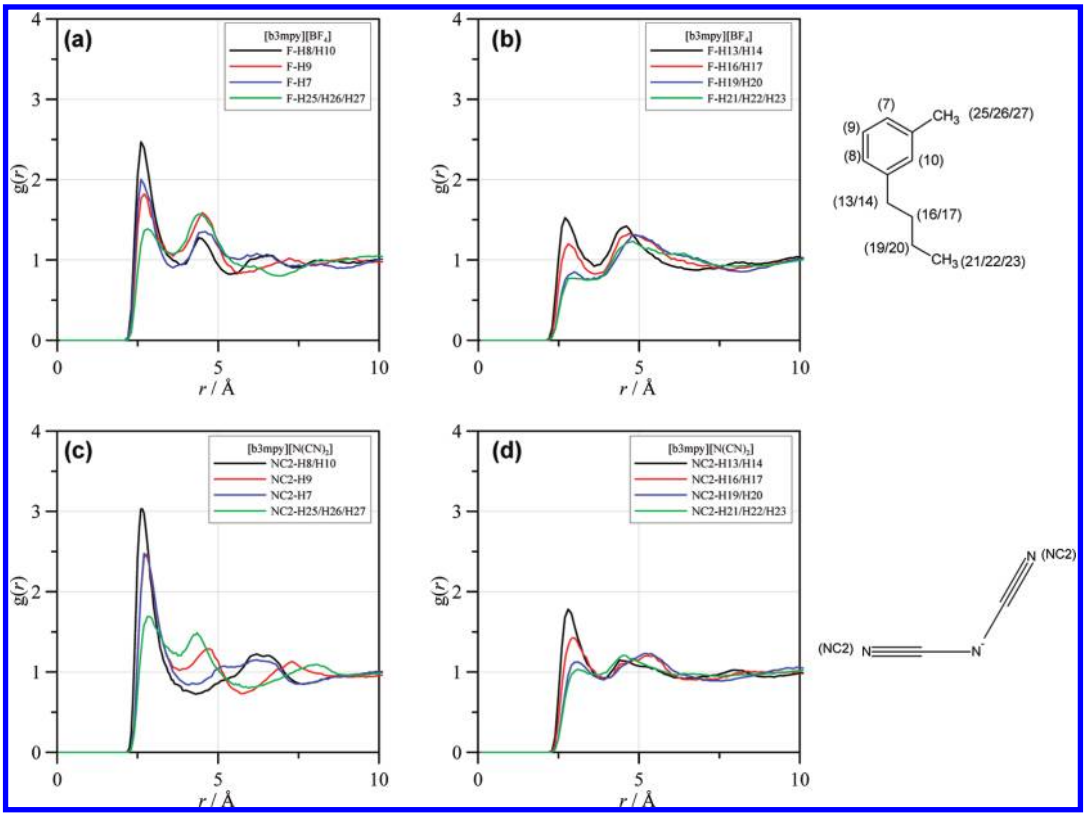

Figure 11. Radial distribution functions, g(r), for pyridinium based ionic liquids at 333 K and 0.1 MPa. $g(r)$s selected show the interaction between the anions and hydrogens along the pyridinium rings to show the ability of hydrogen bonding formation.

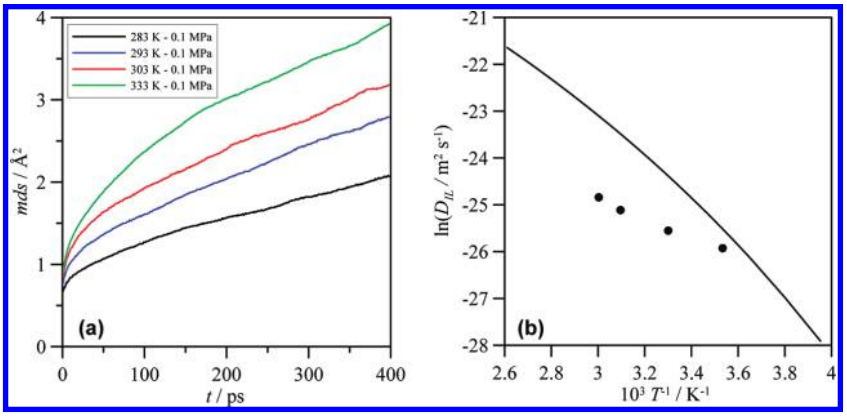

Figure 12. (a) Center-of-mass average mean-square-displacement, msd, and (b) average self−diffusion coefficient (obtained using Einstein's relationship), D, for [bpy][BF_4], as a function of temperature at 0.1 MPa. In panel b we show calculated values (circles) and experimental values (line) obtained from Noda et al.[68] Values are reported as an average of anion and cation data.

agreement with the lower E_{inter} values reported in the previous section, and with the lower viscosity for dicyanamide containing fluids. Cation−cation and anion−anion RDFs show characteristic maxima at almost the distances for which anion−cation RDFs shows minima, and vice versa, which is a clear sign of long-range structuring with alternating cations and anions. Likewise, these peaks are weaker for [b3mpy][$N(CN)_2$].

Electrostatic (Coulombic) interactions are the main factor controlling the molecular level structuring of these ionic liquids, as RDFs and the analysis of energy reported in previous paragraphs show. Nevertheless, van der Waals type interactions are also a remarkable contribution to the total energy of these fluids; therefore, we have analyzed the possibility of hydrogen bonding developing between the anion and cation. We report in Figure 11 RDFs between several possible hydrogen bond donors and acceptors for [b3mpy][BF_4] and [b3mpy][$N(CN)_2$]. We report in Figure 11a RDFs for the interactions between fluorine atoms in BF_4^- cation and all of the hydrogens in [b3mpy]$^+$ anion; these functions show a first narrow and sharp peak with maxima at 2.6 Å, which is in agreement with hydrogen bonding. The intensity of this first peak decreases on going from hydrogen atoms close to the nitrogen atom in the pyridinium ring to hydrogen atoms at

other positions. Nevertheless, the peak appears at the same position for all of the hydrogen atoms in the ring, and thus, hydrogen bonding is developed between the fluorine atoms in the anion and all of the hydrogens in the cation, being most probable with hydrogen close to nitrogen. We have also analyzed the possibility of developing hydrogen bonding between anion fluorine atoms and hydrogens along the alkylic chain in the cation, Figure 11b. The results show a peak at 2.6 Å, the intensity of which decreases on going from the hydrogen atoms in the alkylic chain close to the nitrogen atom toward atoms along the chain. Therefore, hydrogen bonding seems to be possible between fluorine atoms and alkylic hydrogen close to nitrogen. Analogous results are obtained for the interaction between $[b3mpy]^+$ and $[N(CN)_2]^-$ ions, and hydrogen bonding is developed through terminal nitrogens in dicyanamide ion (NC2 atoms), preferentially with hydrogens close to cation nitrogen atom, Figures 11c and d. Therefore, hydrogen bonding is developed among the studied cations and anions and should be a remarkable contribution to the total energy of these systems.

We have also analyzed the dynamic behavior of the studied fluids through the predicted self-diffusion coefficients, D, obtained from molecular dynamics simulations using the Einstein's relationship, eq 11

$$D = \frac{1}{6}\lim_{t\to\infty}\frac{\mathrm{d}}{\mathrm{d}t}\langle \Delta r(t)^2\rangle \tag{11}$$

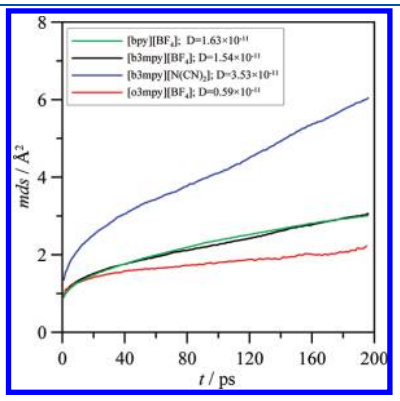

Figure 13. Center-of-mass average mean-square-displacement, msd, and average self−diffusion coefficient (obtained using Einstein's relationship), D, for pyridinium-based ionic liquids, at 333 K and 0.1 MPa.

Where the quantity in brackets is mean square displacement, msd. Long simulations are required to obtain reliable D values from msd results due to the sluggish behavior of ionic liquids.[65] β parameter, defined according to eq 12,[65,66] is very useful to analyze if the diffusive regime has been reached in the evolution of msd with time, and thus, to infer if calculated D values are accurate.

$$\beta(t) = \frac{\mathrm{d}\log_{10}\langle \Delta r(t)^2\rangle}{\mathrm{d}\log_{10} t} \tag{12}$$

Three time regimes for ion translation are obtained: (i) a ballistic regime is obtained ($\beta = 2$) at short times (usually lower than 2 ps), (ii) after this first regime a plateau, corresponding to a subdiffusive regime (with β in the 0.5 − 0.8 range) extending up to large simulation times, and (iii) then, a linear regime with $\beta = 1$, corresponding to a fully diffusive regime, is obtained for the longest times. To compare D values obtained from simulations with experimental values, a fully diffusive regime should be reached in the simulations. A recent work by Roy et al.[67] has showed that simulations for imidazolium-based ionic liquids reach fully diffusive regime for temperatures lower than 350 K from time >10 ns. Moreover, Cadena et al.[52] have showed that pyridinium-based ionic liquids do not reach fully diffusive regime even after 5 ns long simulations. Therefore, as simulations were extended in this work up to 10 ns, D values reported from molecular dynamics simulations should be considered as "apparent" values, obtained from molecular level situations in which ions are trapped in local cages formed by surrounding ions, and thus, these apparent values should be lower than experimental ones. This is confirmed by the β values obtained in this work, which are in the 0.7−0.8 range for all the simulations. Nevertheless, as the objective of the work is to analyze the molecular level mobility of the involved ions, and the factors that control this mobility, and thus, the viscosity, information about the trends between these apparent D values for studied pyridinium-based ionic liquid may be inferred. It has been reported in the literature that ionic liquids travel in pairs, or clusters, both for imidazolium[67] and pyridinium-based fluids,[52] and thus, *msd* and D values are very similar for anion and cation in a fixed ionic liquid. Moreover, Noda et al.[68] measured D values for [bpy]-$[BF_4]$, and obtained similar values for the involved anion and cation, which confirm coupled ionic mobility. Therefore, as the

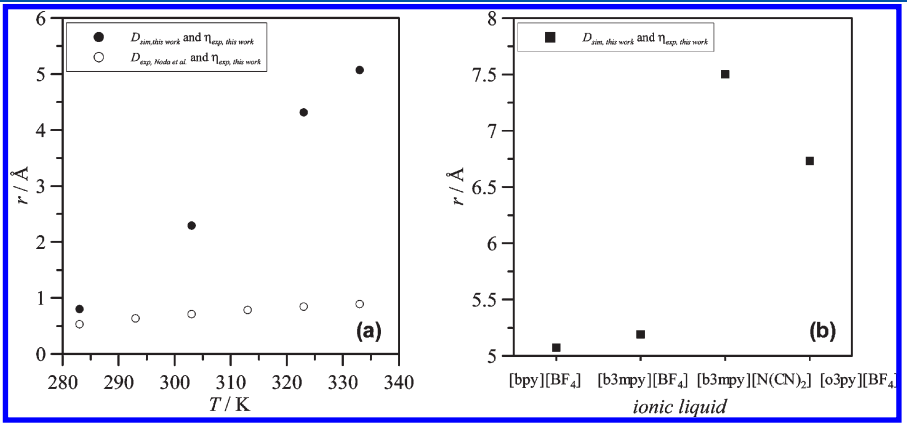

Figure 14. Effective radii, r, of the Stokes−Einstein relationship, calculated for (a) [bpy][BF4] at 0.1 MPa as function of temperature and (b) pyridinium-based ionic liquids at 333 K/0.1 MPa. In panel a, we show r values calculated from experimental viscosity data obtained in this work together with experimental self-diffusion coefficients from Noda et al.[68] and from simulated (subdiffusive regime) self-diffusion coefficients obtained in this work.

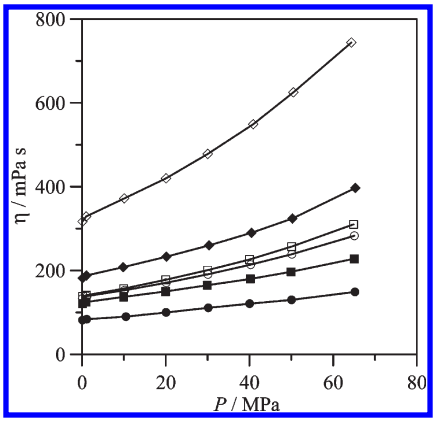

Figure 15. Pressure effect on viscosity for pyridinium-based ionic liquids with common $[BF_4]^-$ anion, at 303.15 K. Symbols: (●) [ppy]-$[BF_4]$; (■) [bpy]$[BF_4]$; (◆) [b2mpy]$[BF_4]$; (○) [b3mpy]$[BF_4]$; (□) [b4mpy]$[BF_4]$; (Δ); and (◇) [o3mpy]$[BF_4]$. Continuous lines show fits for guiding purposes.

objective is to analyze fluids' viscosity, and this is related to D values of the whole fluids, we have studied the changes of average D coefficients (cation and anion average) to analyze whole fluid molecular mobility. We report in Figure 12 msd for [bpy]$[BF_4]$ as a function of temperature for isobaric conditions, and a comparison between the predicted and available experimental D values. Figure 12a shows an increase in *msd* with increasing temperature as we may expect that leads to an increase in D coefficients. Nevertheless, simulated D values are lower than experimental ones, which is caused by the subdiffusive regime for all the simulations (β = 0.7−0.8 range).

We report in Figure 13 calculated D values for the four simulated ionic liquids at isobaric−isothermal conditions, and simulated data are in agreement with experimental viscosity trends: the less viscous fluid, [b3mpy]$[N(CN)_2]$ diffuses faster and the most viscous fluid, [o3mpy]$[BF_4]$ diffuses slower. To the best of our knowledge no experimental D data are available, with the exception of [bpy]$[BF_4]$, and thus, no comparison is possible. Nevertheless, we may expect that predicted D values reported in Figure 13 should be lower than experimental ones. The sluggish behavior of the simulated fluids is inferred from the D values reported in Figure 13, specially for the highly viscous [o3mpy]-$[BF_4]$ ionic liquid for which the calculated D value shows a msd of 0.6 Å^2 per ns of simulation.

Noda et al.[68] showed the correlation between viscosity and D coefficient for [bpy]$[BF_4]$ using the Stokes−Einstein relationship, eq 13

$$\eta = \frac{k_B T}{6\pi D r} \tag{13}$$

where k stands for the Boltzmann constant, T is the temperature, c is a constant (in the 4−6 range), and r is the effective hydrodynamic radius. The main problem for the application of eq 13 to ionic liquids is the value of r. Köddermann et al.[69] showed that the existence of micro heterogeneities, especially for low to moderate temperatures, leads to r values, which are temperature dependent (decreasing with decreasing temperature), and thus the Stokes−Einstein equation is not valid for the neat ionic liquids. Moreover, r values are even lower than the values of isolated cations and anions, and thus, it is not fully clarified the origin of these effective radii.[69] We have calculated r values for

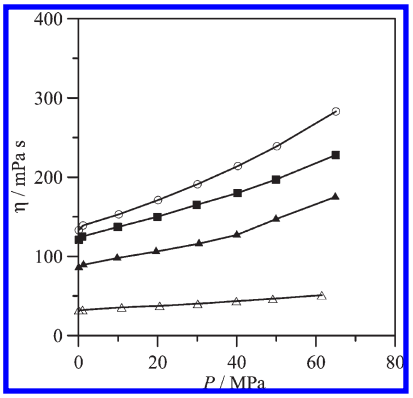

Figure 16. Effect of anion type on pressure effect on viscosity for pyridinium-based ionic, at 303.15 K. Symbols: (■) [bpy]$[BF_4]$; (▲) [bpy]$[CF_3SO_3]$; (○) [b3mpy]$[BF_4]$; and (Δ) [b3mpy]$[N(CN)_2]$. Continuous lines show fits for guiding purposes.

pyridinium-based ionic liquids, which are reported in Figure 14. Results reported in Figure 14a show r values for [bpy]$[BF_4]$ as a function of temperature obtained from experimental viscosity data and experimental and simulated self-diffusion coefficients, and the obtained r values show a too large temperature dependence, which is a consequence of the subdiffusive regime used for the calculation of self-diffusion coefficients. r values obtained from experimental properties are clearly lower than those obtained from simulated D values. Moreover, these values increase with increasing temperature, which was reported by Köddermann et al.[69] for imidazolium-based ionic liquids, and thus, the Stokes−Einstein relationship is not fulfilled by the studied pyridinium-based ionic liquids. The molecular level interpretation of r values is not obvious; we report in Figure 14b calculated r values for the four simulated ionic liquids at the highest simulation temperature, and these values increase with increasing fluids viscosity with the exception of [b3mpy]-$[N(CN)_2]$, which show a remarkably large effective radius. Therefore, r values are not a direct reflection of involved ions sizes, and thus, they should show the characteristics of the micro heterogeneities present in these fluids.

3.4. Analysis of Pressure Effect on Viscosity. We report in Table S2 and Figures S5 and S6 (Supporting Information) the α_η and β_η coefficients obtained from experimental viscosity data. These coefficients measure the effect of pressure and temperature on fluids' viscosity. We analyze in Figure 15 the cation effect on the experimental high-pressure viscosity data for a common anion ($[BF_4]^-$). The rate of increase in viscosity with pressure is greater for the most viscous fluids; at 333.15 K (Figure 15 data) viscosity increases on going from 0.1 to 65 MPa 135%, 125%, 113%, 118%, 88%, and 82% for [o3mpy]$[BF_4]$], [b4mpy]$[BF_4]$, [b3mpy]$[BF_4]$, [b2mpy]$[BF_4]$, [bpy]$[BF_4]$, and [ppy]$[BF_4]$, respectively. Therefore, cations containing longer alkylic chains in the pyridinium cation, or more than one alkylic chain in the cation, are more sensitive to pressure changes.

The effect of anion type on fluids' viscosity is reported in Figure 16. For ionic liquids with $[bpy]^+$ cation, viscosity ordering is $[BF_4]^- > [CF_3SO_3]^-$, but the rate of viscosity increase with pressure is larger for $[CF_3SO_3]^-$ containing ionic liquid (104% and 88% on going from 0.1 to 65 MPa). For ionic liquids with $[b3mpy]^+$ cation, viscosity ordering is $[BF_4]^- > [N(CN)_2]^-$, with remarkably lower viscosity values and rate of viscosity increase (59% on going from 0.1 to 65 MPa) for $[N(CN)_2]^-$ containing ionic liquid.

4. CONCLUSIONS

An experimental and computational study is reported in this work to analyze the viscosity of eight pyridinium-based ionic liquids with several types of anions and cations selected to infer how the structure of involved ions leads to fluids' viscosity. Experimental viscosity measurements were performed in wide pressure temperature ranges, from which pressure and temperature coefficients were calculated for the eight ionic liquids. Viscosity data was analyzed using hole theory, quantum chemistry calculations, and classical molecular dynamics simulations. The application of hole theory leads to successful correlation but with the use of radii different from those calculated from anion and cation sizes. Moreover, the presence of some outliers in the model results points to additional effects not included in the model. Quantum chemistry calculations show a balance between ions sizes and cation/anion interactions strength that, although were tried to relate with viscosity values, could not be properly used to justify viscosity values, mainly because of the conformational flexibility of studied cations, not considered in this work. Classical molecular dynamics simulations show also that intermolecular interaction energy, both electrostatic plus van der Waals types, which is directly defined by geometric factors, may be related with fluids viscosity, with a remarkable role developed by the small cavities size distribution in the ionic liquids. We consider the prevailing role of intermolecular interaction energies together with cavities distribution on fluids viscosity, but these effects are not simple, and thus further studies are required to develop predictive models and structure−property relationships.

■ ASSOCIATED CONTENT

Supporting Information. Figure S1 (comparison of measurements for viscosity standard oil), Figure S2 (comparison between measurements performed with electromagnetic and rolling ball viscometers), Figure S3 (comparison between viscosity values reported in this work and literature data at atmospheric pressure), Table S1 (experimental dynamic viscosity as a function of pressure and temperature), Table S2 (temperature and pressure coefficients), Table S3 (forcefield parameters used for molecular dynamics simulations), Figure S4 (optimized pairs obtained from DFT calculations), Figure S5 (pressure viscosity coefficients), and Figure S6 (temperature viscosity coefficients). This material is available free of charge via the Internet at http://pubs.acs.org.

■ AUTHOR INFORMATION

Corresponding Author
*E-mail: sapar@ubu.es.

■ ACKNOWLEDGMENT

Financial support by Ministerio de Ciencia e Innovación, Spain, (Projects CTQ2009-09458 and CTQ2010-15871) is gratefully acknowledged.

■ REFERENCES

(1) Freemantle, M. *An Introduction to Ionic Liquids*; Royal Society of Chemistry: London, 2010.
(2) Lancaster, M. *Green Chemistry: An Introductory Text*; Royal Society of Chemistry: London, 2010.
(3) Kerton, F. M. *Alternative Solvents for Green Chemistry*; Royal Society of Chemistry: London, 2009.
(4) Plechkova, N. V.; Sedon, K. R. *Chem. Soc. Rev.* **2008**, *37*, 123.
(5) Kirchner, B., Ed.; Ionic Liquids. *Topics in Current Chemistry*; Springer: New York, 2009; Vol. 290.
(6) Giernoth, R. *Angew. Chem., Int. Ed.* **2010**, *49*, 2834.
(7) Wang, Q.; Wu, X. M.; Zhang, D. Y. *Mod. Phys. Lett. B* **2010**, *24*, 1487.
(8) Maginn, E. *J. Phys.: Condens. Matter* **2009**, *21*, 373101.
(9) Weingärtner, H. *Angew. Chem., Int. Ed.* **2008**, *47*, 654.
(10) Aparicio, S.; Atilhan, M.; Karadas, F. *Ind. Eng. Chem. Res.* **2010**, *49*, 9580.
(11) Yamaguchi, T.; Miyake, S.; Koda, S. *J. Phys. Chem. B* **2010**, *114*, 8126.
(12) Pensado, A. S.; Comuñas, M. J. P.; Fernandez, J. *Tribol. Lett.* **2008**, *31*, 107.
(13) Ahosseini, A.; Scurto, A. M. *Int. J. Thermophys.* **2008**, *29*, 1222.
(14) Gao, H.; Luo, M.; Xing, J.; Wu, Y.; Li, Y.; Liu, Q.; Liu, H. *Ind. Eng. Chem. Res.* **2008**, *47*, 8384.
(15) Meinsderma, G. W.; Podt, A.; de Haan, A. B. *Fuel Process. Technol.* **2005**, *87*, 59.
(16) Albrecht, M.; Stoeckli-Evans, H. *Chem. Commun.* **2005**, 4705.
(17) Xiao, Y. *Study or Organic Reactions in Pyridinium-Based ionic liquids*, Ph.D. Thesis; New Jersey Institute of Technology, 2006.
(18) Crosthwaite, J. M.; Muldoon, M. J.; Dixon, J. K.; Anderson, J. L.; Brennecke, J. F. *J. Chem. Thermodyn.* **2005**, *37*, 559.
(19) Nunes, V. M. B., Lourenco, M. J. V.; Santos, F. J. V.; Lopes, M. L. S. M.; Nieto de Castro, C. A. In *Molten Salts and Ionic Liquids. Never the Twain?*; Gaune-Escard, M., Seddon, K. R., Eds.; John Wiley and Sons: New York, 2010.
(20) Nieto de Castro, C. A.; Santos, F. J. V.; Fareleira, J. M. N. A.; Wakeham, W. A. *J. Chem. Eng. Data* **2009**, *54*, 171.
(21) Ahosseini, A.; Scurto, A. M. *Fluid Phase Equilib.* **2009**, *286*, 72.
(22) Aparicio, S.; Alcalde, R.; Garcia, B.; Leal, J. M. J. *Phys. Chem. B* **2009**, *113*, 5593.
(23) Abbott, A. P. *ChemPhysChem* **2004**, *5*, 1242.
(24) Abbott, A. P.; Capper, G.; Gray, S. *ChemPhysChem* **2006**, *7*, 803.
(25) Mokhtarani, B.; Sharifi, A.; Mortaheb, H. R.; Mirzaei, M.; Mafi, M.; Sadeghian, F. *J. Chem. Thermodyn.* **2009**, *41*, 323.
(26) Bandrés, I.; Royo, F. M.; Gascón, I.; Castro, M.; Lafuente, C. *J. Phys. Chem. B* **2010**, *114*, 3601.
(27) Noda, A.; Hayamizu, K.; Watanabe, M. *J. Phys. Chem. B* **2001**, *105*, 4603.
(28) Navas, A.; Ortega, J.; Vreekamp, R.; Marrero, E.; Palomar, J. *Ind. Eng. Chem. Res.* **2009**, *48*, 2678.
(29) Bandrés, I.; Pera, G.; Martín, S.; Castro, M.; Lafuente, C. *J. Phys. Chem. B* **2009**, *113*, 11936.
(30) Crosthwaite, J. M.; Muldoon, M. J.; JaNeille, K.; Dixon, K.; Anderson, J. L.; Brennecke, J. F. *J. Chem. Thermodyn.* **2005**, *37*, 559.
(31) Bandrés, I.; Giner, B.; Artigas, H.; Royo, F. M.; Lafuente, C. *J. Phys. Chem. B* **2008**, *112*, 3077.
(32) Galán, L.; Ribé, J.; Onink, F.; Meindersma, G. W.; de Haan, A. *J. Chem. Eng. Data* **2009**, *54*, 2803.
(33) Bandrés, I.; Giner, B.; Gascón, I.; Castro, M.; Lafuente, C. *J. Phys. Chem. B* **2008**, *112*, 12461.
(34) Bandrés, I.; Giner, B.; Artigas, H.; Lafuente, C.; Royo, F, M. *J. Chem. Eng. Data* **2009**, *54*, 236.
(35) Comuñas, M. J. P.; Baylaucq, A.; Boned, C.; Fernández, J. *Int. J. Thermophys.* **2001**, *22*, 749.
(36) Frisch, M. J.; Trucks, G. W.; Schlegel, H. B.; Scuseria, G. E.; Robb, M. A.; Cheeseman, J. R.; Montgomery, Jr., J. A.; Vreven, T.; Kudin, K. N.; Burant, J. C.; Millam, J. M.; Iyengar, S. S.; Tomasi, J.; Barone, V.; Mennucci, B.; Cossi, M.; Scalmani, G.; Rega, N.; Petersson, G. A.; Nakatsuji, H.; Hada, M.; Ehara, M.; Toyota, K.; Fukuda, R.; Hasegawa, J.; Ishida, M.; Nakajima, T.; Honda, Y.; Kitao, O.; Nakai, H.; Klene, M.; Li, X.; Knox, J. E.; Hratchian, H. P.; Cross, J. B.; Adamo, C.; Jaramillo, J.; Gomperts, R.; Stratmann, R. E.; Yazyev, O.; Austin, A. J.;

Cammi, R.; Pomelli, C.; Ochterski, J. W.; Ayala, P. Y.; Morokuma, K.; Voth, G. A.; Salvador, P.; Dannenberg, J. J.; Zakrzewski, V. G.; Dapprich, S.; Daniels, A. D.; Strain, M. C.; Farkas, O.; Malick, D. K.; Rabuck, A. D.; Raghavachari, K.; Foresman, J. B.; Ortiz, J. V.; Cui, Q.; Baboul, A. G.; Clifford, S.; Cioslowski, J.; Stefanov, B. B.; Liu, G.; Liashenko, A.; Piskorz, P.; Komaromi, I.; Martin, R. L.; Fox, D. J.; Keith, T.; Al-Laham, M. A.; Peng, C. Y.; Nanayakkara, A.; Challacombe, M.; Gill, P. M. W.; Johnson, B.; Chen, W.; Wong, M. W.; Gonzalez, C.; Pople, J. A. *Gaussian 03*, revision C.02; Gaussian, Inc.: Wallingford, CT, 2004.

(37) Becke, A. D. *Phys. Rev. A* **1988**, *38*, 3098.

(38) Lee, C.; Yang, W.; Parr, R. G. *Phys. Rev. B* **1988**, *37*, 785.

(39) Becke, A. D. *J. Chem. Phys.* **1993**, *98*, 5648.

(40) Singh, U. C.; Kollman, P. A. *J. Comput. Chem.* **1984**, *5*, 129.

(41) Besler, B. H.; Merz, K. M.; Kollman, P. A. *J. Comput. Chem.* **1990**, *11*, 431.

(42) Simon, S.; Duran, M.; Dannenberg, J. J. *Chem. Phys.* **1996**, *105*, 11024.

(43) Bader, R. F. W. *Atoms in Molecules: a Quantum Theory*; Oxford University Press: Oxford, U.K., 1990.

(44) Biegler-König, F.; Schönbohm, J.; Bayles, D. *J. Comput. Chem.* **2001**, *22*, 545.

(45) Ponder, J. W. *TINKER: Software tool for molecular design*. 4.2 ed, Washington University School of Medicine, 2004.

(46) Hoover, W. G. *Phys. Rev. A* **1985**, *31*, 1695.

(47) Allen, M. P., Tildesley, D. J., Eds.; *Computer Simulation of Liquids*; Clarendon Press: Oxford, U.K., 1989.

(48) Essmann, U. L.; Perera, M. L.; Berkowitz, T.; Darden, H.; Lee, H.; Pedersen, L. G. *J. Chem. Phys.* **1995**, *103*, 8577.

(49) Martínez, J. M.; Martínez, L. *J. Comput. Chem.* **2003**, *24*, 819–825.

(50) Maginn, E. J. *J. Phys.: Condens. Matter* **2009**, *21*, 373101.

(51) Jorgensen, W. L.; Maxwell, D. S.; Tirado−Rives, J. *J. Am. Chem. Soc.* **1996**, *118*, 11225.

(52) Cadena, C.; Zhao, Q.; Snurr, R. Q.; Maginn, E. J. *J. Phys. Chem. B* **2006**, *110*, 2821.

(53) Canongia-Lopes, J. N.; Pádua, A. H. *J. Phys. Chem. B* **2006**, *110*, 19586.

(54) Suzuki, S.; Shinoda, W.; Saito, H.; Mikami, M.; Tokuda, H.; Watanabe, M. *J. Phys. Chem. B* **2009**, *113*, 10641.

(55) Koch, U.; Popelier, P. L. A. *J. Phys. Chem.* **1995**, *99*, 9747.

(56) Popelier, P. L. A. *J. Phys. Chem. A* **1998**, *102*, 1873.

(57) Sun, H.; Qiao, B.; Zhang, D.; Liu, C. *J. Phys. Chem. A* **2010**, *114*, 3990.

(58) Togichi, K.; Yamamoto, H. *J. Phys. Chem. C* **2007**, *111*, 15989.

(59) Köddermann, T.; Pachek, D.; Ludwig, R. *ChemPhysChem* **2008**, *9*, 549.

(60) Deyko, A.; Lovelock, R. J.; Corfield, J. A.; Taylor, A. W.; Gooden, P. N.; Villa, I. J.; Licence, P.; Jones, R. G.; Krasovskiy, V. G.; Chernikova, E. A.; Kistov, L. M. *Phys. Chem. Chem. Phys.* **2009**, *11*, 8544.

(61) Emelyanenko, V. N.; Vereckin, S. P.; Heintz, A. *Thermochim. Acta* **2011**, in press, DOI: 10.1016/j.tca.2010.11.028

(62) Borodin, O. *J. Phys. Chem. B* **2009**, *113*, 11463.

(63) Borodin, O.; Smith, G. D.; Kim, H. *J. Phys. Chem. B* **2009**, *113*, 4771.

(64) Borodin, O. *J. Phys. Chem. B* **2009**, *113*, 12353.

(65) Del-Popolo, M. G.; Voth, G. A. *J. Phys. Chem. B* **2004**, *108*, 1744.

(66) Hu, Z.; Margulis, C. *Proc. Natl. Acad. Sci.* **2006**, *103*, 831.

(67) Roy, D.; Patel, N.; Conte, S.; Maroncelli, M. *J. Phys. Chem. B* **2010**, *114*, 8410.

(68) Noda, A.; Hayamizu, K.; Watanabe, M. *J. Phys. Chem. B* **2001**, *105*, 4603.

(69) Köddermann, T.; Ludwig, R.; Paschek, D. *ChemPhysChem.* **2008**, *9*, 1851.